

# Nonlinear Robust Optimization for Planning and Control

Arshiya Taj Abdul, Augustinos D. Saravanos and Evangelos A. Theodorou

**Abstract**—This paper presents a novel robust trajectory optimization method for constrained nonlinear dynamical systems subject to unknown bounded disturbances. In particular, we seek optimal control policies that remain robustly feasible with respect to all possible realizations of the disturbances within prescribed uncertainty sets. To address this problem, we introduce a bi-level optimization algorithm. The outer level employs a trust-region successive convexification approach which relies on linearizing the nonlinear dynamics and robust constraints. The inner level involves solving the resulting linearized robust optimization problems, for which we derive tractable convex reformulations and present an Augmented Lagrangian method for efficiently solving them. To further enhance the robustness of our methodology on nonlinear systems, we also illustrate that potential linearization errors can be effectively modeled as unknown disturbances as well. Simulation results verify the applicability of our approach in controlling nonlinear systems in a robust manner under unknown disturbances. The promise of effectively handling approximation errors in such successive linearization schemes from a robust optimization perspective is also highlighted.

## I. INTRODUCTION

Safety-critical trajectory optimization problems arise in a wide range of application domains, including autonomous driving [1], [2], unmanned aerial vehicles [3], [4], multi-agent systems [5], [6], and many other fields. Such systems are often subject to complex nonlinear dynamics and underlying uncertainties, which pose major challenges in designing algorithms that are both robust and computationally efficient. Therefore, there is a great need for optimization frameworks that can effectively handle nonlinear dynamics, guarantee robust and safe operation under uncertainty, and maintain computational tractability.

In most trajectory optimization approaches that explicitly address uncertainty, this is typically achieved through modeling as stochastic noise. Conventional approaches that belong in this category include LQG control [7]–[9], covariance steering [10]–[14] and chance-constrained trajectory optimization algorithms [15]–[18]. Nevertheless, these methods can only guarantee safety and constraint satisfaction in a probabilistic sense. This limitation makes them often impractical for safety-critical applications that require robustness guarantees under *all* possible uncertainty realizations.

This work was supported by the ARO Award #W911NF2010151. Augustinos Saravanos acknowledges financial support by the A. Onassis Foundation Scholarship.

Arshiya Taj Abdul and Augustinos D. Saravanos are with the School of Electrical and Computer Engineering, Georgia Institute of Technology, Atlanta, GA, 30332, USA. {aabdul6, asaravanos}@gatech.edu

Evangelos A. Theodorou is with the Daniel Guggenheim School of Aerospace Engineering, Georgia Institute of Technology, Atlanta, GA, 30332, USA. evangelos.theodorou@gatech.edu

Another approach for characterizing uncertainty is through unknown deterministic disturbances, modeled to lie inside prescribed bounded sets. This approach facilitates the development of trajectory optimization frameworks that guarantee safety and feasibility for all realizations of disturbances by optimizing for the worst-case scenario. This concept originated from the field of *robust control* [19], [20], which focuses on establishing stability and performance margins of control systems under parametric or exogenous uncertainties characterized as unknown deterministic disturbances [21].

Despite the rising interest for achieving robust policies under uncertainty, relatively few works address the challenges of nonlinear dynamics and constraints. One class of related methods is min-max optimal control [22], [23], where the uncertainty is characterized using an adversarial control policy modeled to lie inside a bounded set. However, such robust trajectory optimization methods fail to accommodate state constraints, which are crucial for establishing robustness in safety-critical applications. From a different point of view, robust model predictive control (MPC) typically focuses on linear systems [24], [25]. Tube-based methods are also widely used, yet their main disadvantage is conservatism due to decoupling the nominal control computation from the disturbance rejection [26]. Consequently, there is a critical need for developing optimization frameworks that effectively address constrained nonlinear trajectory optimization problems under unknown disturbances.

Robust Optimization (RO) focuses on finding optimal solutions that remain robust feasible under all possible uncertainty realizations within some prescribed bounded sets [20], [27]. As such problems are inherently intractable due to the semi-infinite nature of the constraints, the main objective of RO techniques is to derive tractable reformulations or approximations. While there exists a rich amount of literature on applying RO methodologies on convex conic optimization problems [27], [28], extending these approaches to settings involving nonlinear/non-convex constraints remains a significant challenge [29]. This difficulty has naturally limited the applicability of RO in trajectory optimization, where nonlinear dynamics and constraints are prevalent.

The contribution of this paper is a novel robust trajectory optimization methodology which extends RO for constrained nonlinear dynamical systems under unknown disturbances. In particular, we present a bi-level optimization framework. The outer level consists of a sequential convexification scheme which linearizes the dynamics and constraints. At the inner level, we address the resulting linearized RO problems by deriving tractable convex reformulations and solving them using an Augmented Lagrangian (AL) method. Furthermore,

we also highlight the ability of our framework to model potential linearization errors as disturbances for further enhancing its robustness on nonlinear systems. We showcase the efficacy and robustness of the proposed methodology through simulation experiments. We also analyze the impact of linearization error on the constraint violation highlighting the effectiveness of modeling through a RO perspective.

*Organization of the Paper:* We begin by introducing the problem statement addressed in this work in Section II. Next, we present the successive linearization scheme in Section III, followed by a methodology for solving the inner robust optimization problems in Section IV. In Section V, we provide the complete algorithm for our robust nonlinear trajectory optimization framework. We then extend the framework to incorporate linearization error as uncertainty in Section VI. The efficiency of the proposed frameworks is illustrated through simulation experiments in Section VII. Section VIII concludes our paper and provides future research directions.

*Notations:* We represent the space of symmetric positive definite (semidefinite) matrices with dimension  $n$  as  $\mathbb{S}_n^{++}$  ( $\mathbb{S}_n^+$ ). The 2-norm of a vector  $\mathbf{x}$  is denoted with  $\|\mathbf{x}\|_2$ , while the Frobenius norm of a matrix  $\mathbf{X}$  is given by  $\|\mathbf{X}\|_F$ . Further, a weighted 2-norm of a vector  $\mathbf{x}$  defined for a  $\mathbf{Q} \in \mathbb{S}_n^+$  as  $\sqrt{\mathbf{x}^T \mathbf{Q} \mathbf{x}}$  is denoted by  $\|\mathbf{x}\|_{\mathbf{Q}}$ . The indicator function of a set  $X$ ,  $\mathcal{I}_X$  is defined as  $\mathcal{I}(x) = \{0 \text{ if } x \in X \text{ or } +\infty \text{ if } x \notin X\}$ . With  $\llbracket a, b \rrbracket$ , we denote the integer set  $\{[a, b] \cap \mathbb{Z}\}$ .

## II. PROBLEM STATEMENT

Consider the following discrete-time nonlinear dynamics

$$\begin{aligned} \mathbf{x}_{k+1} &= f(\mathbf{x}_k, \mathbf{u}_k) + \mathbf{d}_k, \quad k \in \llbracket 0, T-1 \rrbracket, \\ \mathbf{x}_0 &= \bar{\mathbf{x}}_0 + \bar{\mathbf{d}}_0, \end{aligned} \quad (1)$$

where  $\mathbf{x}_k \in \mathbb{R}^{n_x}$  is the state,  $\mathbf{u}_k \in \mathbb{R}^{n_u}$  is the control input,  $f : \mathbb{R}^{n_x} \times \mathbb{R}^{n_u} \rightarrow \mathbb{R}^{n_x}$  is the known dynamics function and  $T$  is the time horizon. The terms  $\mathbf{d}_k \in \mathbb{R}^{n_x}$  represent *unknown disturbances* which are formally defined below. In addition, the initial state  $\mathbf{x}_0$  consists of a known part  $\bar{\mathbf{x}}_0$ , as well as an unknown part  $\bar{\mathbf{d}}_0$ .

In this work, we characterize the uncertainty to be lying in a bounded ellipsoidal set. This is quite common in most robust control applications, where ellipsoidal sets are used to model exogenous uncertainty [30]. Further, ellipsoidal sets can form a basis to address other more complex uncertainty sets [31]. Considering  $\boldsymbol{\zeta} = [\bar{\mathbf{d}}_0; \mathbf{d}_0; \dots; \mathbf{d}_{T-1}]$ , we define the uncertainty set

$$\mathcal{U}[\tau] = \{\boldsymbol{\zeta} \mid \exists (\mathbf{z} \in \mathbb{R}^{n_z}, \tau \in \mathbb{R}^+) : \boldsymbol{\zeta} = \mathbf{\Gamma} \mathbf{z}, \mathbf{z}^T \mathbf{S} \mathbf{z} \leq \tau\},$$

where  $\boldsymbol{\zeta} \in \mathbb{R}^{(T+1)n_x}$ ,  $\mathbf{\Gamma} \in \mathbb{R}^{(T+1)n_x \times n_z}$ , and  $\mathbf{S} \in \mathbb{S}_{n_z}^{++}$ . Note that the positive definiteness of the matrix  $\mathbf{S}$  ensures that the uncertainty set is bounded. We also highlight that our methodology can be extended for other common types of uncertainty sets such as ellitopes, polytopes, etc. [20].

Our system is also subject to the following *robust* state and control constraints

$$\mathbf{g}(\mathbf{x}; \boldsymbol{\zeta}) \leq 0, \quad \forall \boldsymbol{\zeta} \in \mathcal{U}[\tau], \quad (3)$$

$$\mathbf{h}(\mathbf{u}; \boldsymbol{\zeta}) \leq 0, \quad \forall \boldsymbol{\zeta} \in \mathcal{U}[\tau], \quad (4)$$

where  $\mathbf{x} = [\mathbf{x}_0; \mathbf{x}_1; \dots; \mathbf{x}_T]$ ,  $\mathbf{u} = [\mathbf{u}_0; \mathbf{u}_1; \dots; \mathbf{u}_{T-1}]$ ,  $\mathbf{g} : \mathbb{R}^{(T+1)n_x} \rightarrow \mathbb{R}^{n_g}$  and  $\mathbf{h} : \mathbb{R}^{Tn_u} \rightarrow \mathbb{R}^{n_h}$ . We emphasize that we seek for solutions that satisfy the above constraints for all possible realizations of the disturbances  $\boldsymbol{\zeta}$  within the uncertainty set  $\mathcal{U}[\tau]$ . In particular, we seek affine control policies of the following form

$$\mathbf{u}_k = \bar{\mathbf{u}}_k + \mathbf{K}_k \mathbf{d}_{k-1}, \quad (5)$$

where  $\bar{\mathbf{u}}_k \in \mathbb{R}^{n_u}$  are feed-forward controls and  $\mathbf{K}_k \in \mathbb{R}^{n_u \times n_x}$  are feedback gains. By convention, we set  $\mathbf{d}_{-1} = \bar{\mathbf{d}}_0$ . We will now introduce the robust trajectory optimization problem addressed in this work.

**Problem 1** (Robust Trajectory Optimization Problem). *Find the optimal control policy  $\{\bar{\mathbf{u}}_k, \mathbf{K}_k\}_{k=0}^{T-1}$  such that*

$$\begin{aligned} \min_{\{\bar{\mathbf{u}}_k, \mathbf{K}_k\}_{k=0}^{T-1}} & \sum_{k=0}^{T-1} \bar{\mathbf{u}}_k^T \mathbf{R}_k \bar{\mathbf{u}}_k + \|\mathbf{R}_k \mathbf{K}_k\|_F^2 \\ \text{s.t.} & \quad \mathbf{x}_{k+1} = f(\mathbf{x}_k, \mathbf{u}_k) + \mathbf{d}_k, \quad \mathbf{x}_0 = \bar{\mathbf{x}}_0 + \bar{\mathbf{d}}_0, \\ & \quad \mathbf{g}(\mathbf{x}; \boldsymbol{\zeta}) \leq 0, \quad \mathbf{h}(\mathbf{u}; \boldsymbol{\zeta}) \leq 0, \quad \forall \boldsymbol{\zeta} \in \mathcal{U}[\tau]. \end{aligned} \quad (6)$$

The above problem is especially challenging because of the following inherent difficulties. First, Problem 1 is not tractable at its current form as it is subject to an infinite amount of constraints. The robust constraints are the constraints that need to be satisfied for all possible realizations of the uncertainty  $\boldsymbol{\zeta}$  lying in the defined uncertainty set  $\mathcal{U}[\tau]$ . The second difficulty stems from the nonlinearity in the dynamics and the constraints which do not allow for the direct application of standard robust optimization (RO) techniques to convert the problem into a tractable form. The following sections present a methodology that integrates robust optimization, successive linearization and operator splitting through the Alternating Direction Method of Multipliers [32] towards effectively addressing these challenges.

## III. SUCCESSIVE LINEARIZATION APPROACH

We start with introducing a successive linearization scheme for addressing the nonlinearities in Problem 1. Let us define the disturbance-free states  $\bar{\mathbf{x}}_k$  whose dynamics are obtained through simply setting  $\boldsymbol{\zeta} = \mathbf{0}$ , i.e.,

$$\bar{\mathbf{x}}_{k+1} = f(\bar{\mathbf{x}}_k, \bar{\mathbf{u}}_k), \quad k \in \llbracket 0, T-1 \rrbracket. \quad (7)$$

Then, the disturbance component  $\mathbf{x}_k^d$  of the state is given by

$$\mathbf{x}_k^d = \mathbf{x}_k - \bar{\mathbf{x}}_k. \quad (8)$$

*1) Dynamics Linearization:* To construct a successive linearization scheme, we consider linearizing the dynamics (1), around a nominal trajectory  $\{\hat{\mathbf{x}}_k, \hat{\mathbf{u}}_k\}_{k=0}^{T-1}$ , whose dynamics are given by

$$\hat{\mathbf{x}}_{k+1} = f(\hat{\mathbf{x}}_k, \hat{\mathbf{u}}_k), \quad k \in \llbracket 0, T-1 \rrbracket, \quad (9)$$

$$\hat{\mathbf{x}}_0 = \bar{\mathbf{x}}_0. \quad (10)$$

Thus, we obtain the following linearized dynamics

$$\mathbf{x}_{k+1} - \hat{\mathbf{x}}_{k+1} = \mathbf{A}_k (\mathbf{x}_k - \hat{\mathbf{x}}_k) + \mathbf{B}_k (\mathbf{u}_k - \hat{\mathbf{u}}_k) + \mathbf{d}_k \quad (11)$$

with  $\mathbf{A}_k \in \mathbb{R}^{n_x \times n_x}$  and  $\mathbf{B}_k \in \mathbb{R}^{n_x \times n_u}$  given as

$$\mathbf{A}_k = \nabla_{\mathbf{x}} f(\mathbf{x}_k, \mathbf{u}_k) \Big|_{\substack{\mathbf{x}_k = \hat{\mathbf{x}}_k \\ \mathbf{u}_k = \hat{\mathbf{u}}_k}}, \quad \mathbf{B}_k = \nabla_{\mathbf{u}} f(\mathbf{x}_k, \mathbf{u}_k) \Big|_{\substack{\mathbf{x}_k = \hat{\mathbf{x}}_k \\ \mathbf{u}_k = \hat{\mathbf{u}}_k}}.$$

Next, we define the deviations  $\delta \hat{\mathbf{x}}_k = \bar{\mathbf{x}}_k - \hat{\mathbf{x}}_k$ ,  $\delta \hat{\mathbf{u}}_k = \bar{\mathbf{u}}_k - \hat{\mathbf{u}}_k$ , such that using (5), (8), we can rewrite (11) as

$$\delta \hat{\mathbf{x}}_{k+1} + \mathbf{x}_{k+1}^d = \mathbf{A}_k(\delta \hat{\mathbf{x}}_k + \mathbf{x}_k^d) + \mathbf{B}_k(\delta \hat{\mathbf{u}}_k + \mathbf{K}_k \mathbf{d}_{k-1}) + \mathbf{d}_k \quad (12)$$

or in a more compact form as

$$\delta \hat{\mathbf{x}} + \mathbf{x}^d = \mathbf{F}_0 \delta \hat{\mathbf{x}}_0 + \mathbf{F}_u(\delta \hat{\mathbf{u}} + \mathbf{K} \boldsymbol{\zeta}) + \mathbf{F}_0 \mathbf{x}_0^d + \mathbf{F}_d \boldsymbol{\zeta} \quad (13)$$

where  $\mathbf{x}^d = [\mathbf{x}_0^d; \dots; \mathbf{x}_T^d]$ ,  $\delta \hat{\mathbf{x}} = [\delta \hat{\mathbf{x}}_0; \dots; \delta \hat{\mathbf{x}}_T]$ ,  $\delta \hat{\mathbf{u}} = [\delta \hat{\mathbf{u}}_0; \dots; \delta \hat{\mathbf{u}}_{T-1}]$ ,  $\mathbf{K} = \text{bdiag}(\{\mathbf{K}_k\}_{k=0}^{T-1})$  and the matrices  $\mathbf{F}_0$ ,  $\mathbf{F}_u$ , and  $\mathbf{F}_d$  are defined in Appendix A. Finally, given that  $\delta \hat{\mathbf{x}}_0 = 0$  and  $\mathbf{x}_0^d = \bar{\mathbf{d}}_0$ , we can further simplify (13) to

$$\delta \hat{\mathbf{x}} + \mathbf{x}^d = \mathbf{F}_u(\delta \hat{\mathbf{u}} + \mathbf{K} \boldsymbol{\zeta}) + \mathbf{F}_d \boldsymbol{\zeta} \quad (14)$$

where the matrix  $\mathbf{F}_\zeta$  is also defined in Appendix A.

2) *Robust Constraints Linearization*: Subsequently, we also linearize the robust constraints. Note that linear constraints, e.g. control box constraints, can be directly incorporated. Without loss of generality, we limit our exposition to the state constraints  $\mathbf{g}(\mathbf{x}; \boldsymbol{\zeta}) \leq 0$ . In particular, we obtain the linearized robust constraint

$$\mathbf{g}(\hat{\mathbf{x}}) + \nabla_{\mathbf{x}} \mathbf{g}(\hat{\mathbf{x}})(\delta \hat{\mathbf{x}} + \mathbf{x}^d) \leq 0, \quad \forall \boldsymbol{\zeta} \in \mathcal{U}[\tau], \quad (15)$$

around the nominal trajectory  $\{\hat{\mathbf{x}}_k, \hat{\mathbf{u}}_k\}_{k=0}^{T-1}$ . By combining the linearized dynamics (12) with (15), we arrive to the equivalent constraint

$$\mathbf{g}^{\text{lin}}(\delta \hat{\mathbf{u}}, \mathbf{K}; \boldsymbol{\zeta}) \leq 0, \quad \forall \boldsymbol{\zeta} \in \mathcal{U}[\tau], \quad (16)$$

where

$$\mathbf{g}^{\text{lin}} = \mathbf{g}(\hat{\mathbf{x}}) + \nabla_{\mathbf{x}} \mathbf{g}(\hat{\mathbf{x}})(\mathbf{F}_u(\delta \hat{\mathbf{u}} + \mathbf{K} \boldsymbol{\zeta}) + \mathbf{F}_d \boldsymbol{\zeta}). \quad (17)$$

3) *Successive Linearization Scheme*: Based on the previous linearizations, we propose an iterative scheme which solves the following problem in place of Problem 1.

**Problem 2** (Linearized Problem). *Find the optimal decision variables  $\delta \hat{\mathbf{u}}, \mathbf{K}$  such that*

$$\min_{\delta \hat{\mathbf{u}}, \mathbf{K}} \mathcal{Q}_{\hat{\mathbf{u}}}(\delta \hat{\mathbf{u}}) + \mathcal{Q}_K(\mathbf{K})$$

$$\text{s.t. } \mathbf{g}^{\text{lin}}(\delta \hat{\mathbf{u}}, \mathbf{K}; \boldsymbol{\zeta}) \leq 0, \quad \forall \boldsymbol{\zeta} \in \mathcal{U}[\tau], \quad (18a)$$

$$\|\mathbf{F}_u \delta \hat{\mathbf{u}}\|_2 \leq r_{\text{trust}}, \quad (18b)$$

where  $\mathcal{Q}_{\hat{\mathbf{u}}}(\delta \hat{\mathbf{u}}) = \sum_{k=0}^{T-1} (\hat{\mathbf{u}}_k + \delta \hat{\mathbf{u}}_k)^T \mathbf{R}_u^k (\hat{\mathbf{u}}_k + \delta \hat{\mathbf{u}}_k)$ ,  $\mathcal{Q}_K(\mathbf{K}) = \sum_{k=0}^{T-1} \|\mathbf{R}_K^k \mathbf{K}_k\|_F^2$ .

The trust region constraint (18b) with  $r_{\text{trust}} \in \mathbb{R}^+$  is added to ensure the boundedness of the linearized problem. The solution of Problem 2 would provide a new nominal trajectory  $\{\hat{\mathbf{x}}_k, \hat{\mathbf{u}}_k\}_{k=0}^{T-1}$  around which we perform a new linearization, and so on - as described in the next section. Nevertheless, we still cannot solve the above problem due to two prominent issues. The first is computational intractability due to the constraint (16), while the second one is temporary infeasibilities that might arise in the linearized problems.

## IV. INNER CONSTRAINED ROBUST OPTIMIZATION

### A. Tractable Reformulation of Robust Optimization Problem

In this section, we transform Problem 2 into tractable form. We start by splitting the constraint (16) through introducing a slack variable  $\mathbf{p} = [p_1; \dots; p_{n_g}] \in \mathbb{R}^{n_g}$ , which leads to the following set of constraints

$$\mathbf{g}^{\text{lin},1}(\delta \hat{\mathbf{u}}, \mathbf{p}) := \mathbf{g}(\hat{\mathbf{x}}) + \nabla_{\mathbf{x}} \mathbf{g}(\hat{\mathbf{x}}) \mathbf{F}_u \delta \hat{\mathbf{u}} + \mathbf{p} \leq 0, \quad (19)$$

$$\mathbf{g}^{\text{lin},2}(\mathbf{K}, \mathbf{p}; \boldsymbol{\zeta}) := \nabla_{\mathbf{x}} \mathbf{g}(\hat{\mathbf{x}})(\mathbf{F}_u \mathbf{K} + \mathbf{F}_d) \boldsymbol{\zeta} \leq \mathbf{p}, \quad \forall \boldsymbol{\zeta} \in \mathcal{U}[\tau]. \quad (20)$$

Note that only the constraint (20) now depends on the uncertainty  $\boldsymbol{\zeta}$ , and thus remains intractable. We transform it into a tractable form by first reformulating it as

$$\max_{\boldsymbol{\zeta} \in \mathcal{U}[\tau]} \nabla_{\mathbf{x}} \mathbf{g}(\hat{\mathbf{x}})(\mathbf{F}_u \mathbf{K} + \mathbf{F}_d) \boldsymbol{\zeta} \leq \mathbf{p}, \quad (21)$$

which implies that the constraint needs to be satisfied for the worst-case scenario. Next, by using the first-order optimality conditions [33], we obtain for each  $j \in \llbracket 1, n_g \rrbracket$ ,

$$\begin{aligned} \max_{\boldsymbol{\zeta} \in \mathcal{U}[\tau]} \nabla_{\mathbf{x}} \mathbf{g}_j(\hat{\mathbf{x}})^T (\mathbf{F}_u \mathbf{K} + \mathbf{F}_d) \boldsymbol{\zeta} \\ = (\tau)^{1/2} \|\mathbf{\Gamma}^T (\mathbf{F}_u \mathbf{K} + \mathbf{F}_d)^T \nabla_{\mathbf{x}} \mathbf{g}_j(\hat{\mathbf{x}})\|_{\mathbf{S}^{-1}}, \end{aligned} \quad (22)$$

using which, the constraint (21) can be equivalently given by the following set of tractable constraints

$$g_j^{\text{trac}}(\mathbf{K}, \mathbf{p}) \leq 0, \quad j \in \llbracket 1, n_g \rrbracket, \quad (23)$$

with

$$g_j^{\text{trac}}(\mathbf{K}, \mathbf{p}) := (\tau)^{1/2} \|\mathbf{\Gamma}^T (\mathbf{F}_u \mathbf{K} + \mathbf{F}_d)^T \nabla_{\mathbf{x}} \mathbf{g}_j(\hat{\mathbf{x}})\|_{\mathbf{S}^{-1}} - p_j.$$

Thus, Problem 2 is equivalent to the following convex tractable reformulation.

**Problem 3** (Tractable Linearized Problem). *Find the optimal decision variables  $\delta \hat{\mathbf{u}}, \mathbf{K}, \mathbf{p}$  such that*

$$\min_{\delta \hat{\mathbf{u}}, \mathbf{K}, \mathbf{p}} \mathcal{Q}_{\hat{\mathbf{u}}}(\delta \hat{\mathbf{u}}) + \mathcal{Q}_K(\mathbf{K})$$

$$\text{s.t. } \mathbf{g}^{\text{lin},1}(\delta \hat{\mathbf{u}}, \mathbf{p}) \leq 0,$$

$$g_j^{\text{trac}}(\mathbf{K}, \mathbf{p}) \leq 0, \quad j \in \llbracket 1, n_g \rrbracket,$$

$$\|\mathbf{F}_u \delta \hat{\mathbf{u}}\|_2 \leq r_{\text{trust}}.$$

### B. ADMM for Solving Constrained Robust Optimization

Subsequently, we present a method for solving Problem 3, based on the Alternating Direction Method of Multipliers (ADMM). ADMM is an AL approach for solving convex optimization problems of the form

$$\min_{\mathbf{y} \in Y, \tilde{\mathbf{y}} \in \tilde{Y}} \mathcal{H}_y(\mathbf{y}) + \mathcal{H}_{\tilde{y}}(\tilde{\mathbf{y}}) \quad \text{s.t. } \mathbf{P} \mathbf{y} + \mathbf{Q} \tilde{\mathbf{y}} = \mathbf{b}, \quad (24)$$

where  $\mathcal{H}_y$  and  $\mathcal{H}_{\tilde{y}}$  are closed, proper, and convex functions [32]. This framework solves the problem in a distributed manner with respect to the variables  $\mathbf{y}$  and  $\tilde{\mathbf{y}}$  (typically referred to as ADMM blocks). However, we are using this algorithm due to its key feature of infeasibility detection [34], [35]. Under certain mild assumptions, if the cost function  $\mathcal{H}_y$  and  $\mathcal{H}_{\tilde{y}}$  are convex quadratic and the matrix  $[\mathbf{P}, \mathbf{Q}]$  has full rank, then the ADMM converges to a solution, lying in

the set  $\{(\mathbf{y}, \tilde{\mathbf{y}}) : \mathbf{y} \in Y, \tilde{\mathbf{y}} \in \tilde{Y}\}$ , that has the minimum Euclidean distance to the set  $\{(\mathbf{y}, \tilde{\mathbf{y}}) : \mathbf{P}\mathbf{y} + \mathbf{Q}\tilde{\mathbf{y}} = \mathbf{b}\}$  [35]. Thus, we can employ ADMM to inexactly solve Problem 3.

To achieve this, we need to first transform Problem 3 to the form (24). For that, we would rewrite the set of constraints (23) using the slack variable  $\tilde{\mathbf{p}} \in \mathbb{R}^{n_g}$  as the following equivalent constraints

$$g_j^{\text{trac}}(\mathbf{K}, \tilde{\mathbf{p}}) \leq 0, \quad j \in \llbracket 1, n_g \rrbracket, \quad (25)$$

$$\mathbf{p} = \tilde{\mathbf{p}}. \quad (26)$$

Thus, Problem 3 can be equivalently expressed in the following form.

**Problem 4** (Tractable Linearized Problem - ADMM form). *Find the optimal decision variables  $\delta\hat{\mathbf{u}}, \mathbf{K}, \mathbf{p}, \tilde{\mathbf{p}}$  such that*

$$\begin{aligned} \min_{\delta\hat{\mathbf{u}}, \mathbf{K}, \mathbf{p}, \tilde{\mathbf{p}}} \quad & \mathcal{H}_p(\delta\hat{\mathbf{u}}, \mathbf{p}) + \mathcal{H}_{\tilde{\mathbf{p}}}(\mathbf{K}, \tilde{\mathbf{p}}) \\ \text{s.t.} \quad & \mathbf{p} = \tilde{\mathbf{p}} \end{aligned}$$

with  $\mathcal{H}_p(\delta\hat{\mathbf{u}}, \mathbf{p}) = \mathcal{I}_{\mathcal{P}} + \mathcal{Q}_{\hat{\mathbf{u}}}(\delta\hat{\mathbf{u}})$ ,  $\mathcal{H}_{\tilde{\mathbf{p}}}(\mathbf{K}, \tilde{\mathbf{p}}) = \mathcal{I}_{\tilde{\mathcal{P}}} + \mathcal{Q}_K(\mathbf{K})$ , where  $\mathcal{P}$  represents the feasible region for the set of constraints (18b), (19), and  $\tilde{\mathcal{P}}$  represents the feasible region for the constraint (25).

To solve Problem 4 using ADMM, we start with formulating the AL as follows

$$\begin{aligned} \mathcal{L}_\rho(\delta\hat{\mathbf{u}}, \mathbf{p}, \mathbf{K}, \tilde{\mathbf{p}}; \boldsymbol{\lambda}) = & \mathcal{H}_p(\delta\hat{\mathbf{u}}, \mathbf{p}) + \mathcal{H}_{\tilde{\mathbf{p}}}(\mathbf{K}, \tilde{\mathbf{p}}) \\ & + \boldsymbol{\lambda}^\top (\mathbf{p} - \tilde{\mathbf{p}}) + \frac{\rho}{2} \|\mathbf{p} - \tilde{\mathbf{p}}\|_2^2, \end{aligned} \quad (27)$$

where  $\boldsymbol{\lambda} \in \mathbb{R}^{n_g}$  is the dual variable for the constraint  $\mathbf{p} = \tilde{\mathbf{p}}$  and  $\rho > 0$  is the penalty parameter. We consider the variables  $\{\mathbf{K}, \tilde{\mathbf{p}}\}$  as the first block, and  $\{\delta\hat{\mathbf{u}}, \mathbf{p}\}$  as the second block of ADMM. Each ADMM iteration - indexed with  $l_{\text{in}}$  - would then involve the following sequential steps:

- i)  $\{\mathbf{K}, \tilde{\mathbf{p}}\}^{l_{\text{in}}} = \underset{\mathbf{K}, \tilde{\mathbf{p}}}{\text{argmin}} \mathcal{L}_\rho(\{\delta\hat{\mathbf{u}}, \mathbf{p}\}^{l_{\text{in}}-1}, \mathbf{K}, \tilde{\mathbf{p}}; \boldsymbol{\lambda}^{l_{\text{in}}-1})$
- ii)  $\{\delta\hat{\mathbf{u}}, \mathbf{p}\}^{l_{\text{in}}} = \underset{\delta\hat{\mathbf{u}}, \mathbf{p}}{\text{argmin}} \mathcal{L}_\rho(\delta\hat{\mathbf{u}}, \mathbf{p}, \{\mathbf{K}, \tilde{\mathbf{p}}\}^{l_{\text{in}}}; \boldsymbol{\lambda}^{l_{\text{in}}-1})$
- iii)  $\boldsymbol{\lambda}^{l_{\text{in}}} = \underset{\boldsymbol{\lambda}}{\text{argmax}} \mathcal{L}_\rho(\{\delta\hat{\mathbf{u}}, \mathbf{p}, \mathbf{K}, \tilde{\mathbf{p}}\}^{l_{\text{in}}}; \boldsymbol{\lambda})$

The above updates can finally be rewritten as follows

$$\begin{aligned} \{\mathbf{K}, \tilde{\mathbf{p}}\}^{l_{\text{in}}} = \underset{\mathbf{K}, \tilde{\mathbf{p}}}{\text{argmin}} \quad & \mathcal{Q}_K(\mathbf{K}) + \boldsymbol{\lambda}^{l_{\text{in}}-1\top} (\mathbf{p}^{l_{\text{in}}-1} - \tilde{\mathbf{p}}) \\ & + \frac{\rho}{2} \|\mathbf{p}^{l_{\text{in}}-1} - \tilde{\mathbf{p}}\|_2^2 \end{aligned} \quad (28a)$$

$$\text{s.t.} \quad g_j^{\text{trac}}(\mathbf{K}, \tilde{\mathbf{p}}) \leq 0, \quad j \in \llbracket 1, n_g \rrbracket,$$

$$\begin{aligned} \{\delta\hat{\mathbf{u}}, \mathbf{p}\}^{l_{\text{in}}} = \underset{\delta\hat{\mathbf{u}}, \mathbf{p}}{\text{argmin}} \quad & \mathcal{Q}_{\hat{\mathbf{u}}}(\delta\hat{\mathbf{u}}) + \boldsymbol{\lambda}^{l_{\text{in}}-1\top} (\mathbf{p} - \tilde{\mathbf{p}}^{l_{\text{in}}}) \\ & + \frac{\rho}{2} \|\mathbf{p} - \tilde{\mathbf{p}}^{l_{\text{in}}}\|_2^2 \end{aligned} \quad (28b)$$

$$\text{s.t.} \quad \mathbf{g}^{\text{lin},1}(\delta\hat{\mathbf{u}}, \mathbf{p}) \leq 0, \quad \|\mathbf{F}_u \delta\hat{\mathbf{u}}\|_2 \leq r_{\text{trust}},$$

$$\boldsymbol{\lambda}^{l_{\text{in}}} = \boldsymbol{\lambda}^{l_{\text{in}}-1} + \rho(\mathbf{p}^{l_{\text{in}}} - \tilde{\mathbf{p}}^{l_{\text{in}}}). \quad (28c)$$

---

### Algorithm 1 Nonlinear Robust Trajectory Optimization

---

**Input:** Uncertainty set parameters  $\mathbf{S}, \tau, \bar{\mathbf{x}}_0$

*Initialization:*  $\hat{\mathbf{u}}, \rho, \boldsymbol{\lambda}, \mathbf{p}, \tilde{\mathbf{p}}, r_{\text{trust}}, \alpha \in [0.5, 1), \beta > 1, \eta_1, \eta_2, r_{\text{min}}, \rho_{\text{max}} \in \mathbb{R}^+$

- 1: **while not converged do**
- 2:   Set the nominal trajectory  $(\hat{\mathbf{x}}, \hat{\mathbf{u}})$  :
- 3:    $\hat{\mathbf{x}}_0 = \bar{\mathbf{x}}_0$ ,
- 4:   **for**  $k = 0$  to  $T - 1$  **do**
- 5:      $\hat{\mathbf{x}}_{k+1} = f(\hat{\mathbf{x}}_k, \hat{\mathbf{u}}_k)$
- 6:   **end for**
- 7:   Solve the Problem 3 linearized around  $(\hat{\mathbf{x}}, \hat{\mathbf{u}})$  :
- 8:   **if**  $\|\mathbf{p} - \tilde{\mathbf{p}}\|_2 \leq \epsilon_p$  **then**
- 9:     Solve Problem 3  $\leftarrow \delta\hat{\mathbf{u}}, \mathbf{K}$ .
- 10:     $\mathbf{p} = \tilde{\mathbf{p}}$
- 11:   **else**
- 12:     Inexactly solve Problem 4 using the Algorithm 2  $\leftarrow \delta\hat{\mathbf{u}}, \mathbf{K}, \boldsymbol{\lambda}, \mathbf{p}, \tilde{\mathbf{p}}$
- 13:   **end if**
- 14:    $\hat{\mathbf{u}} = \hat{\mathbf{u}} + \delta\hat{\mathbf{u}}$
- 15:   **if**  $\|\delta\hat{\mathbf{u}}\|_2 \leq \epsilon_{\hat{\mathbf{u}}}$  and  $\mathbf{p} = \tilde{\mathbf{p}}$  **then**
- 16:     break
- 17:   **end if**
- 18:   **if**  $\|\delta\hat{\mathbf{u}}\|_2 \geq \eta_1 \|\mathbf{p} - \tilde{\mathbf{p}}\|_2$  **then**
- 19:     reduce  $r_{\text{trust}}$ :  $r_{\text{trust}} = \min(\alpha r_{\text{trust}}, r_{\text{min}})$
- 20:   **else if**  $\|\delta\hat{\mathbf{u}}\|_2 \leq \eta_2 \|\mathbf{p} - \tilde{\mathbf{p}}\|_2$  **then**
- 21:     Increase  $\rho$ :  $\rho = \max(\beta\rho, \rho_{\text{max}})$
- 22:   **end if**
- 23: **end while**

**Output:**  $\hat{\mathbf{u}}, \mathbf{K}$

---



---

### Algorithm 2 Inner ADMM Loop

---

**Input:**  $\boldsymbol{\lambda}, \mathbf{p}, \tilde{\mathbf{p}}, \rho$

- 1: *Initialize*  $\boldsymbol{\lambda}^0 = \boldsymbol{\lambda}, \mathbf{p}^0 = \mathbf{p}, \tilde{\mathbf{p}}^0 = \tilde{\mathbf{p}}$
- 2: **for**  $l_{\text{in}} = 1$  to  $L_{\text{max}}^{\text{in}}$  **do**
- 3:   Sequentially solve (28a), (28b), and (28c)
- 4:   **if**  $\|\mathbf{p}^{l_{\text{in}}} - \tilde{\mathbf{p}}^{l_{\text{in}}}\|_2 \leq \epsilon_p$  **then**
- 5:     break
- 6:   **end if**
- 7: **end for**
- 8:  $\delta\hat{\mathbf{u}} = \delta\hat{\mathbf{u}}^{l_{\text{in}}}, \mathbf{K} = \mathbf{K}^{l_{\text{in}}}$
- 9:  $\mathbf{p} = \mathbf{p}^{l_{\text{in}}}, \tilde{\mathbf{p}} = \tilde{\mathbf{p}}^{l_{\text{in}}}, \boldsymbol{\lambda} = \boldsymbol{\lambda}^{l_{\text{in}}}$

**Output:**  $\delta\hat{\mathbf{u}}, \mathbf{K}, \mathbf{p}, \tilde{\mathbf{p}}, \boldsymbol{\lambda}$

---

## V. FINAL ALGORITHM

In this section, we combine the above techniques to present the complete version of the bi-level optimization framework in Algorithm 1. First, the nominal control  $\hat{\mathbf{u}}$ , penalty parameter  $\rho$ , dual variable  $\boldsymbol{\lambda}$ , and slack variables  $\mathbf{p}$  and  $\tilde{\mathbf{p}}$  need to be initialized. In each outer iteration, we linearize Problem 1 around the nominal trajectory  $\{\hat{\mathbf{x}}_k, \hat{\mathbf{u}}_k\}_{k=0}^{T-1}$  to obtain Problem 3. Nevertheless, as discussed earlier, Problem 3 can be infeasible. Thus, for the initial outer iterations, Problem 4 (an equivalent version of Problem 3) is inexactly solved using ADMM as disclosed in Algorithm 2. This involves sequentially solving (28a), (28b), and (28c) for a

set number of ADMM iterations  $L_{\max}^{\text{in}}$ . This approach is continued until the residual  $\|\mathbf{p} - \tilde{\mathbf{p}}\|_2$  falls below a set threshold  $\epsilon_p > 0$ . Once this happens, in each outer iteration, Problem 3 is directly solved to obtain  $\delta\hat{\mathbf{u}}$ ,  $\mathbf{K}$ . Further, in each outer iteration, the trust region radius  $r_{\text{trust}}$  and the penalty parameter  $\rho$  are updated using the parameters  $\alpha$  and  $\beta$  respectively, based on the residuals  $\|\delta\hat{\mathbf{u}}\|_2$  and  $\|\mathbf{p} - \tilde{\mathbf{p}}\|_2$ . The algorithm is terminated when the following convergence criteria are fulfilled

$$\|\delta\hat{\mathbf{u}}\|_2 \leq \epsilon_{\hat{\mathbf{u}}} \text{ and } \mathbf{p} = \tilde{\mathbf{p}} \quad (29)$$

where  $\epsilon_{\hat{\mathbf{u}}} > 0$  is a set threshold.

Note that it is possible that the above framework would still not provide a completely robust solution for the actual nonlinear system as it relies on linearization techniques which might contain approximation errors. In the subsequent section, we address this challenge by presenting an extension of this framework which also models the linearization errors through a RO point of view.

## VI. LINEARIZATION ERROR AS UNCERTAINTY

In this section, we present an extension of the above proposed framework to address the approximation errors that arise in successive linearization schemes. Note that Algorithm 1 ensures that a *linearized* trajectory given as

$$\mathbf{x}^{\text{lin}} = \bar{\mathbf{x}} + \mathbf{x}^d = \bar{\mathbf{x}} + (\mathbf{F}_u \mathbf{K} + \mathbf{F}_\zeta) \boldsymbol{\zeta} \quad (30)$$

satisfies all the constraints in the robust sense. However, this might not ensure that the actual trajectory  $\mathbf{x}$  would satisfy all the constraints due to the linearization error (i.e.,  $\mathbf{x} - \mathbf{x}^{\text{lin}}$ ). This reveals the need for ensuring robustness even in the presence of such linearization errors. For that, we interpret the linearization error as an additional source of uncertainty, such that we have the following instead of (14)

$$\delta\hat{\mathbf{x}} + \mathbf{x}^d = \mathbf{F}_u(\delta\hat{\mathbf{u}} + \mathbf{K}\boldsymbol{\zeta}) + \mathbf{x}^e \quad (31)$$

where  $\mathbf{x}^e \in \mathbb{R}^{(T+1)n_x}$  is the linearization error defined as  $\mathbf{x}^e = [\mathbf{x}_0^e; \mathbf{x}_1^e; \dots; \mathbf{x}_T^e]$ , with each of its components  $\mathbf{x}_k^e$  lying in the following ellipsoidal uncertainty sets

$$\mathcal{E}^k[\tau_k^e] = \{\mathbf{x}_k^e \in \mathbb{R}^{n_x} \mid \exists (\mathbf{e}_k^c \in \mathbb{R}^{n_x}, \tau_k^e \in \mathbb{R}^+) : (\mathbf{x}_k^e - \mathbf{e}_k^c)^T \mathbf{S}_k^e (\mathbf{x}_k^e - \mathbf{e}_k^c) \leq \tau_k^e\}, \quad (32)$$

where  $\mathbf{S}_k^e \in \mathbb{S}_{n_x}^{++}$ . We incorporate this modification into Algorithm 1 by replacing the set of constraints (25) with

$$g_j^{\text{trac}}(\mathbf{K}, \tilde{\mathbf{p}}) + \nabla_{\mathbf{x}} \mathbf{g}_j(\hat{\mathbf{x}})^T \mathbf{x}^e \leq 0 \quad \forall \{\mathbf{x}_k^e \in \mathcal{E}^k\}_{k=0}^T. \quad (33)$$

Then, we have

$$\nabla_{\mathbf{x}} \mathbf{g}_j(\hat{\mathbf{x}})^T \mathbf{x}^e = \sum_{k=0}^T \nabla_{\mathbf{x}_k} \mathbf{g}_j(\hat{\mathbf{x}})^T \mathbf{x}_k^e, \quad (34)$$

using which, we can rewrite the constraint (33) as follows

$$g_j^{\text{trac}}(\mathbf{K}, \tilde{\mathbf{p}}) + \sum_{k=0}^T \max_{\mathbf{x}_k^e \in \mathcal{E}^k} \nabla_{\mathbf{x}_k} \mathbf{g}_j(\hat{\mathbf{x}})^T \mathbf{x}_k^e \leq 0. \quad (35)$$

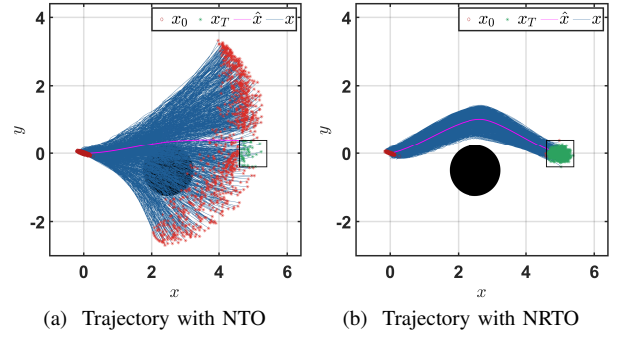


Fig. 1. **NTO vs. NRTO**: Only 2 out of 1000 trajectory realizations obtained using NTO satisfy all the constraints. While only 3 out of 1000 trajectory realizations obtained using NRTO violate the constraints.

Let us now simplify  $\max_{\mathbf{x}_k^e \in \mathcal{E}^k} \nabla_{\mathbf{x}_k} \mathbf{g}_j(\hat{\mathbf{x}})^T \mathbf{x}_k^e$  by defining a variable  $\tilde{\mathbf{x}}_k^e = \mathbf{x}_k^e - \mathbf{e}_k^c$  such that we obtain

$$\begin{aligned} \max_{\mathbf{x}_k^e \in \mathcal{E}^k} \nabla_{\mathbf{x}_k} \mathbf{g}_j(\hat{\mathbf{x}})^T \mathbf{x}_k^e \\ = \nabla_{\mathbf{x}_k} \mathbf{g}_j(\hat{\mathbf{x}})^T \mathbf{e}_k^c + \max_{\tilde{\mathbf{x}}_k^e \in \mathcal{E}_k^e} \nabla_{\mathbf{x}_k} \mathbf{g}_j(\hat{\mathbf{x}})^T \tilde{\mathbf{x}}_k^e. \end{aligned} \quad (36)$$

By using the first order optimality conditions, we get

$$\max_{\tilde{\mathbf{x}}_k^e \in \mathcal{E}_k^e} \nabla_{\mathbf{x}_k} \mathbf{g}_j(\hat{\mathbf{x}})^T \tilde{\mathbf{x}}_k^e = (\tau_k^e)^{1/2} \|\nabla_{\mathbf{x}_k} \mathbf{g}_j(\hat{\mathbf{x}})\|_{(\mathbf{S}_k^e)^{-1}} \quad (37)$$

Using (36) and (37), we can then rewrite (35) as follows

$$g_j^{\text{trac}}(\mathbf{K}, \tilde{\mathbf{p}}) + g_j^{\text{err}} \leq 0 \quad (38)$$

where

$$g_j^{\text{err}} = \sum_{k=0}^T \left[ \nabla_{\mathbf{x}_k} \mathbf{g}_j(\hat{\mathbf{x}})^T \mathbf{e}_k^c + (\tau_k^e)^{1/2} \|\nabla_{\mathbf{x}_k} \mathbf{g}_j(\hat{\mathbf{x}})\|_{(\mathbf{S}_k^e)^{-1}} \right].$$

The extension of Algorithm 1 for treating the linearization error as uncertainty, can be given by replacing the constraints (25) in Algorithm 1 with the constraints (38).

## VII. SIMULATION RESULTS

In this section, we demonstrate the effectiveness of the proposed frameworks. Throughout this section, we refer to Algorithm 1 without considering the linearization errors as **NRTO**, and to the extension for handling linearization errors as disclosed in Section VI as **NRTO-LE**. All simulations were carried out in Matlab2022b [36] environment using YALMIP [37] as the modeling software and MOSEK [38] as the solver on a system with an Intel Core9-13900K.

We initially consider a unicycle model with state  $[x; y; \theta]$ , and control inputs  $[v; \omega]$ , where  $(x, y)$  and  $\theta$  represent the 2D position and angle respectively, while  $v$  and  $\omega$  represent the linear and angular velocities. The dynamics are provided in Appendix B. We consider a time horizon of  $T = 30$  with a step size  $\Delta t = 0.01s$ , and the uncertainty set parameters  $\mathbf{S} = \mathbf{I}$ , with  $\Gamma$  and uncertainty level  $\tau$  varying across the cases. The matrix  $\Gamma$  is randomly generated in each case with each element  $\Gamma_{ij} = \text{unifrnd}(-1, 1)$ .

First, we demonstrate the effectiveness of our robust framework in Fig. 1. We consider a non-robust variant of

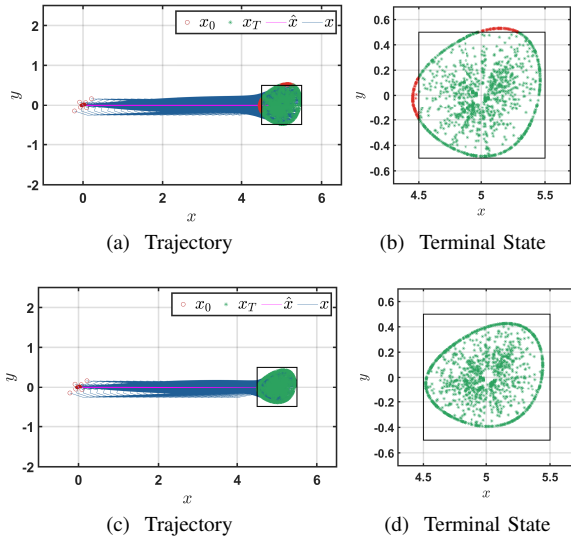


Fig. 2. **Performance Comparison between NRTO and NRTO-LE:** Uncertainty level is set to  $\tau = 0.1$ . (a) and (b) correspond to the NRTO, with 92.1% constraint satisfaction. (c) and (d) correspond to the NRTO-LE, with 100% constraint satisfaction.

the framework NRTO, referred to as **NTO**, wherein the trajectory optimization problem is solved *without* accounting for the disturbance  $\zeta$  (i.e., implementing NRTO with  $\tau = 0$ ). For NRTO, we consider a case with an uncertainty level  $\tau = 0.05$ . The task requires the unicycle to reach the target position bounds (shown by the black box) while avoiding the circular obstacle. Fig. 1 shows 1000 trajectory realizations obtained using each framework NTO and NRTO. Fig. 1a shows that using NTO, only a few reach the target position bounds (green markers inside the bounds). Further, only two realizations satisfy all the constraints (i.e., obstacle and terminal state constraints). On the other hand, using NRTO, as shown in Fig. 1b, all the trajectory realizations avoid the obstacle, and 99.7% of them reach the target position bounds. Therefore, NRTO significantly improves constraint satisfaction over its non-robust variant (NTO), thereby enhancing the reliability of the system under uncertainty.

As observed earlier in Fig. 1b, a few trajectory realizations obtained using NRTO still violate the terminal state constraints, which is due to the linearization error. Since the obstacle constraints involve concave functions - whose linearizations yield more conservative constraints - the effect of the linearization error is not that pronounced for these constraints. However, the effect can be observed for the terminal position constraints — and it could be further amplified for models with stronger nonlinearities. In the following, we analyze the effect of the linearization error and highlight the effectiveness of NRTO-LE in guaranteeing robustness. In Fig. 2, we consider a case with an uncertainty level  $\tau = 0.1$  and with the target position constraints as shown. Fig. 2a and 2b show the trajectory and terminal state realizations obtained using NRTO, while Fig. 2c and 2d show those obtained with NRTO-LE. Using NRTO only yields 92.1% constraint satisfaction, with a few terminal

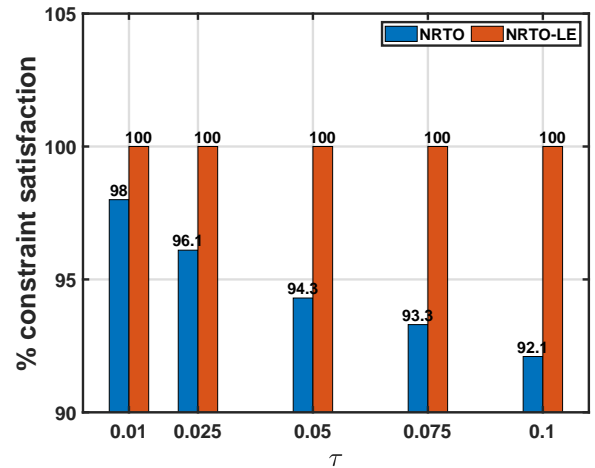


Fig. 3. **Uncertainty vs. Constraint Satisfaction:** Comparison of percentage of constraint satisfaction over 1500 realizations using NRTO and NRTO-LE. The constraint satisfaction decreases with increase in uncertainty using the NRTO, while NRTO-LE provides 100% constraint satisfaction in all the cases.

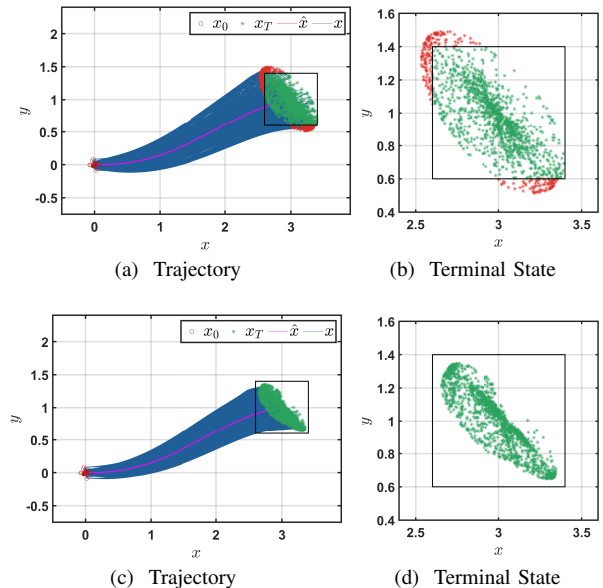


Fig. 4. **Performance Comparison between NRTO and NRTO-LE for car model:** Uncertainty level is set to  $\tau = 0.01$ . (a) and (b) correspond to the NRTO, with 84.2% constraint satisfaction. (c) and (d) correspond to the NRTO-LE, with 100% constraint satisfaction.

state realizations outside the target position bounds (red markings). To address this, we characterize the linearization error as disclosed in Section VI based on the trajectory realizations obtained using NRTO. In particular, we construct confidence ellipsoids from the aforementioned observed data to define the linearization error uncertainty sets of the form (33). Note that these linearization error uncertainty sets can also be constructed using other more sophisticated methods [39]. Fig. 2c and 2d show that, using NRTO-LE, none of the trajectory realizations violate the target position bounds, highlighting the robustness of the proposed approach.

We further emphasize the effectiveness of NRTO-LE over

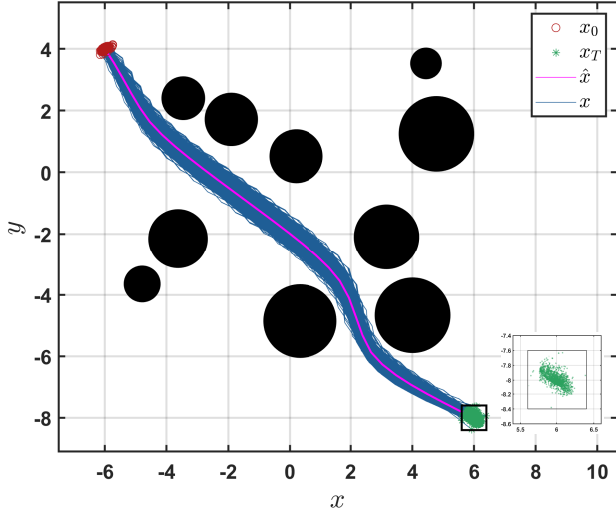


Fig. 5. **Complex scenario for unicycle with ten obstacles using NRTO-LE:** Uncertainty level is set to  $\tau = 0.05$ . 100% constraint satisfaction considering 1500 trajectory realizations.

NRTO by comparing their performance over increasing levels of uncertainty and nonlinearity. In Fig. 3, we analyze the effect of the uncertainty level  $\tau$  on the constraint satisfaction. This analysis considers the same task as in Fig. 2 with the same  $\Gamma$  and target position bounds. It can be observed that using NRTO, constraint satisfaction decreases with increasing levels of uncertainty. In contrast, NRTO-LE leverages the data obtained from the NRTO output and consistently provides 100% constraint satisfaction. In Fig. 4, we consider a more complex 2D car model with state  $[x; y; \theta; v]$  and control inputs  $[\omega; a]$ . The state components  $(x, y)$  represent the position of the midpoint of the back axle,  $\theta$  represents the car's orientation, and  $v$  represents the velocity of the front wheels. The control components  $\omega$  and  $a$  represent the angle and acceleration of the front wheels. The full dynamics are provided in Appendix B. We consider a time horizon  $T = 50$  with a step size  $\Delta t = 0.03s$ . The designated task requires the car to reach the target position bounds as shown in Fig. 4, and the terminal angle  $\theta_T$  to be constrained within  $[-1, 1]$ . Fig. 4a and 4b correspond to NRTO, and Fig. 4c and 4d correspond to NRTO-LE. In both cases, there is no violation of the terminal angle constraint (i.e.,  $\theta_T \in [-1, 1]$ ), yet, using NRTO, a considerable amount of realizations end up outside of the target position bounds — with only 84.2% of them satisfying the constraints. On the other hand, the NRTO-LE approach provided 100% constraint satisfaction.

Lastly, we demonstrate the effectiveness of NRTO-LE in handling complex navigation tasks, as shown in Fig. 5. This task involves a unicycle which is required to reach the target position bounds while avoiding ten circular obstacles under an uncertainty level of  $\tau = 0.05$ . Fig. 5 illustrates that none of the 1500 realizations violate any of the constraints.

## VIII. CONCLUSION

We propose a novel, robust nonlinear trajectory optimization framework capable of handling nonlinear and nonconvex

constraints. We leverage robust optimization (RO) techniques by effectively integrating them with sequential linearization schemes and an ADMM approach. Additionally, we effectively address the linearization error arising in such schemes by modeling it as a deterministic disturbance. Our NRTO-LE framework demonstrates 100% constraint satisfaction in all studied cases and maintains its effectiveness for more complex scenarios.

In future work, we plan to extend the current framework for nonlinear robust MPC under unknown disturbances to handle dynamically evolving environments. We also aim to explore distributed optimization approaches for scaling our methodology to large-scale multi-agent systems [33]. Another promising direction would be investigating data-driven frameworks for estimating the uncertainty sets [40], [41] as well as for accelerating the underlying ADMM method [42], towards further enhancing the robustness and scalability of the proposed approach.

## APPENDIX

### A. Linearized Dynamics matrices

The matrices  $\mathbf{F}_0$ ,  $\mathbf{F}_u$ ,  $\mathbf{F}_d$  and  $\mathbf{F}_\zeta$  are given as

$$\mathbf{F}_0 = \begin{bmatrix} \mathbf{I}; & \Phi(1, 0); & \Phi(2, 0); & \ddots; & \Phi(N, 0) \end{bmatrix},$$

$$\mathbf{F}_u = \begin{bmatrix} \mathbf{0} & \mathbf{0} & \dots & \mathbf{0} \\ \mathbf{B}_0 & \mathbf{0} & \dots & \mathbf{0} \\ \Phi(2, 1)\mathbf{B}_0 & \mathbf{B}_1 & \dots & \mathbf{0} \\ \vdots & \vdots & \vdots & \vdots \\ \Phi(N, 1)\mathbf{B}_0 & \Phi(N, 2)\mathbf{B}_1 & \dots & \mathbf{B}_{N-1} \end{bmatrix},$$

$$\tilde{\mathbf{F}}_d = \begin{bmatrix} \mathbf{0} & \mathbf{0} & \dots & \mathbf{0} \\ \mathbf{I} & \mathbf{0} & \dots & \mathbf{0} \\ \Phi(2, 1) & \mathbf{I} & \dots & \mathbf{0} \\ \vdots & \vdots & \vdots & \vdots \\ \Phi(N, 1) & \Phi(N, 2) & \dots & \mathbf{I} \end{bmatrix},$$

$$\mathbf{F}_d = \begin{bmatrix} \mathbf{0} & \tilde{\mathbf{F}}_d \end{bmatrix}, \quad \mathbf{F}_\zeta = \begin{bmatrix} \mathbf{F}_0, \tilde{\mathbf{F}}_d \end{bmatrix},$$

where  $\Phi(k_1, k_2) = \mathbf{A}_{k_1-1}\mathbf{A}_{k_1-2}\dots\mathbf{A}_{k_2}$  for  $k_1 > k_2$ .

### B. Simulation Dynamical models

Here, we provide the models used in our simulations.

a) *Unicycle Model:* The unicycle dynamics are

$$\begin{aligned} x_{k+1} &= x_k + v_k \cos(\theta_k)\Delta t, \\ y_{k+1} &= y_k + v_k \sin(\theta_k)\Delta t, \\ \theta_{k+1} &= \theta_k + \omega_k\Delta t. \end{aligned}$$

b) *Car model:* For the 2D car, the distance between the front and rear axles of car is  $c_{\text{len}} = 0.75$ . The rolling distances of the front and back wheels are  $c_k^f = v_k\Delta t$  and

$$c_k^b = c_k^f \cos(\omega_k) + c_{\text{len}} + \sqrt{c_{\text{len}}^2 - (c_k^f \cos(\omega_k))^2},$$

respectively. The dynamics are then given as

$$\begin{aligned} x_{k+1} &= x_k + c_k^b \cos(\theta_k), & y_{k+1} &= y_k + c_k^b \sin(\theta_k), \\ \theta_{k+1} &= \theta_k + \arcsin\left(\sin(\omega_k) \frac{c_k^f}{c_{\text{len}}}\right), \\ v_{k+1} &= v_k + a_k\Delta t. \end{aligned}$$

## REFERENCES

- [1] T. A. Howell, B. E. Jackson, and Z. Manchester, "Altro: A fast solver for constrained trajectory optimization," in *2019 IEEE/RSJ International Conference on Intelligent Robots and Systems (IROS)*. IEEE, 2019, pp. 7674–7679.
- [2] Y. Aoyama, O. So, A. D. Saravanos, and E. A. Theodorou, "Second-order constrained dynamic optimization," *arXiv preprint arXiv:2409.11649*, 2024.
- [3] R. Bonalli, A. Cauligi, A. Bylard, and M. Pavone, "Gusto: Guaranteed sequential trajectory optimization via sequential convex programming," in *2019 International Conference on Robotics and Automation (ICRA)*, 2019, pp. 6741–6747.
- [4] H. Oleynikova, M. Burri, Z. Taylor, J. Nieto, R. Siegwart, and E. Galceran, "Continuous-time trajectory optimization for online uav replanning," in *2016 IEEE/RSJ international conference on intelligent robots and systems (IROS)*. IEEE, 2016, pp. 5332–5339.
- [5] A. D. Saravanos, Y. Aoyama, H. Zhu, and E. A. Theodorou, "Distributed differential dynamic programming architectures for large-scale multiagent control," *IEEE Transactions on Robotics*, vol. 39, no. 6, pp. 4387–4407, 2023.
- [6] O. Shorinwa and M. Schwager, "Distributed model predictive control via separable optimization in multiagent networks," *IEEE Transactions on Automatic Control*, vol. 69, no. 1, pp. 230–245, 2023.
- [7] E. Todorov and W. Li, "A generalized iterative lqg method for locally-optimal feedback control of constrained nonlinear stochastic systems," in *Proceedings of the 2005, American Control Conference, 2005*. IEEE, 2005, pp. 300–306.
- [8] J. Chen, Y. Shimizu, L. Sun, M. Tomizuka, and W. Zhan, "Constrained iterative lqg for real-time chance-constrained gaussian belief space planning," in *2021 IEEE/RSJ International Conference on Intelligent Robots and Systems (IROS)*. IEEE, 2021, pp. 5801–5808.
- [9] J. Ma, Z. Cheng, X. Zhang, Z. Lin, F. L. Lewis, and T. H. Lee, "Local learning enabled iterative linear quadratic regulator for constrained trajectory planning," *IEEE Transactions on Neural Networks and Learning Systems*, vol. 34, no. 9, pp. 5354–5365, 2022.
- [10] J. Ridderhof, K. Okamoto, and P. Tsiotras, "Nonlinear uncertainty control with iterative covariance steering," in *2019 IEEE 58th Conference on Decision and Control (CDC)*, 2019, pp. 3484–3490.
- [11] K. Okamoto and P. Tsiotras, "Optimal stochastic vehicle path planning using covariance steering," *IEEE Robotics and Automation Letters*, vol. 4, no. 3, pp. 2276–2281, 2019.
- [12] F. Liu, G. Rapakoulis, and P. Tsiotras, "Optimal covariance steering for discrete-time linear stochastic systems," *IEEE Transactions on Automatic Control*, 2024.
- [13] I. M. Balci, E. Bakolas, B. Vlahov, and E. A. Theodorou, "Constrained covariance steering based tube-mppi," in *2022 American Control Conference (ACC)*. IEEE, 2022, pp. 4197–4202.
- [14] A. D. Saravanos, I. M. Balci, E. Bakolas, and E. A. Theodorou, "Distributed model predictive covariance steering," in *2024 IEEE/RSJ International Conference on Intelligent Robots and Systems (IROS)*, 2024, pp. 5740–5747.
- [15] T. Lew, R. Bonalli, and M. Pavone, "Chance-constrained sequential convex programming for robust trajectory optimization," in *2020 European Control Conference (ECC)*, 2020, pp. 1871–1878.
- [16] Y. K. Nakka and S.-J. Chung, "Trajectory optimization of chance-constrained nonlinear stochastic systems for motion planning under uncertainty," *IEEE Transactions on Robotics*, vol. 39, no. 1, pp. 203–222, 2023.
- [17] Y. K. Nakka, A. Liu, G. Shi, A. Anandkumar, Y. Yue, and S.-J. Chung, "Chance-constrained trajectory optimization for safe exploration and learning of nonlinear systems," *IEEE Robotics and Automation Letters*, vol. 6, no. 2, pp. 389–396, 2020.
- [18] Y. Aoyama, A. D. Saravanos, and E. A. Theodorou, "Receding horizon differential dynamic programming under parametric uncertainty," in *2021 60th IEEE Conference on Decision and Control (CDC)*, 2021, pp. 3761–3767.
- [19] M. G. Safonov, "Origins of robust control: Early history and future speculations," *IFAC Proceedings Volumes*, vol. 45, no. 13, pp. 1–8, 2012, 7th IFAC Symposium on Robust Control Design. [Online]. Available: <https://www.sciencedirect.com/science/article/pii/S1474667015376540>
- [20] A. Ben-Tal, A. Nemirovski, and L. El Ghaoui, "Robust optimization," 2009.
- [21] M. Green and D. J. Limebeer, *Linear robust control*. Courier Corporation, 2012.
- [22] J. Morimoto and C. Atkeson, "Minimax differential dynamic programming: An application to robust biped walking," *Advances in neural information processing systems*, vol. 15, 2002.
- [23] W. Sun, Y. Pan, J. Lim, E. A. Theodorou, and P. Tsiotras, "Minimax differential dynamic programming: Continuous and discrete time formulations," *Journal of Guidance, Control, and Dynamics*, vol. 41, no. 12, pp. 2568–2580, 2018.
- [24] A. Richards and J. How, "Robust model predictive control with imperfect information," in *Proceedings of the 2005, American Control Conference, 2005*. IEEE, 2005, pp. 268–273.
- [25] J. Oravec and M. Bakošová, "Alternative lmi-based robust mpc design approaches," *IFAC-PapersOnLine*, vol. 48, no. 14, pp. 180–185, 2015.
- [26] D. Q. Mayne, E. C. Kerrigan, and P. Falugi, "Robust model predictive control: advantages and disadvantages of tube-based methods," *IFAC Proceedings Volumes*, vol. 44, no. 1, pp. 191–196, 2011.
- [27] A. Ben-Tal and A. Nemirovski, "Robust optimization—methodology and applications," *Mathematical programming*, vol. 92, pp. 453–480, 2002.
- [28] D. Bertsimas, D. B. Brown, and C. Caramanis, "Theory and applications of robust optimization," *SIAM review*, vol. 53, no. 3, pp. 464–501, 2011.
- [29] S. Leyffer, M. Menickelly, T. Munson, C. Vanaret, and S. M. Wild, "A survey of nonlinear robust optimization," *INFOR: Information Systems and Operational Research*, vol. 58, no. 2, pp. 342–373, 2020.
- [30] I. R. Petersen, V. A. Ugrinovskii, and A. V. Savkin, *Introduction*. London: Springer London, 2000, pp. 1–18.
- [31] A. Ben-Tal and A. Nemirovski, "Robust solutions of uncertain linear programs," *Operations Research Letters*, vol. 25, no. 1, pp. 1–13, 1999. [Online]. Available: <https://www.sciencedirect.com/science/article/pii/S0167637799000164>
- [32] S. Boyd, N. Parikh, E. Chu, B. Peleato, J. Eckstein *et al.*, "Distributed optimization and statistical learning via the alternating direction method of multipliers," *Foundations and Trends® in Machine Learning*, vol. 3, no. 1, pp. 1–122, 2011.
- [33] A. T. Abdul, A. D. Saravanos, and E. A. Theodorou, "Scaling robust optimization for multi-agent robotic systems: A distributed perspective," *arXiv preprint arXiv:2402.16227*, 2024.
- [34] G. Banjac, P. Goulart, B. Stellato, and S. Boyd, "Infeasibility detection in the alternating direction method of multipliers for convex optimization," *Journal of Optimization Theory and Applications*, vol. 183, pp. 490–519, 2019.
- [35] A. U. Raghunathan and S. Di Cairano, "Infeasibility detection in alternating direction method of multipliers for convex quadratic programs," in *53rd IEEE Conference on Decision and Control*, 2014, pp. 5819–5824.
- [36] T. M. Inc., "Matlab version: 9.13.0 (r2022b)," Natick, Massachusetts, United States, 2022. [Online]. Available: <https://www.mathworks.com>
- [37] J. Lofberg, "Yalmip: A toolbox for modeling and optimization in matlab," in *2004 IEEE international conference on robotics and automation (IEEE Cat. No. 04CH37508)*. IEEE, 2004, pp. 284–289.
- [38] M. ApS, *The MOSEK optimization toolbox for MATLAB manual. Version 9.0.*, 2019. [Online]. Available: <http://docs.mosek.com/9.0/toolbox/index.html>
- [39] I. Alon, D. Arnon, and A. Wiesel, "Learning minimal volume uncertainty ellipsoids," *IEEE Signal Processing Letters*, vol. 31, pp. 1655–1659, 2024.
- [40] D. Bertsimas, V. Gupta, and N. Kallus, "Data-driven robust optimization," *Mathematical Programming*, vol. 167, pp. 235–292, 2018.
- [41] I. Wang, C. Becker, B. Van Parys, and B. Stellato, "Learning decision-focused uncertainty sets in robust optimization," *arXiv preprint arXiv:2305.19225*, 2023.
- [42] A. D. Saravanos, H. Kuperman, A. Oshin, A. T. Abdul, V. Pacelli, and E. Theodorou, "Deep distributed optimization for large-scale quadratic programming," in *The Thirteenth International Conference on Learning Representations*, 2025. [Online]. Available: <https://openreview.net/forum?id=hzuumhfYSO>